Decay of the excited compound system ^{56}Ni* formed through various channels using deformed Coulomb and deformed nuclear proximity potentials

K. P. Santhosh* and P. V. Subha

School of Pure and Applied Physics, Kannur University, Swami Anandatheertha Campus, Payyanur 670327, Kerala, India

(Received 26 January 2017; revised manuscript received 3 May 2017; published 12 June 2017)

The total cross section, the intermediate mass fragment (IMF) production cross section, and the cross section for the formation of light particles (LPs) for the decay of compound system ^{56}Ni* formed through the entrance channel ^{32}S + ^{24}Mg have been evaluated by taking the scattering potential as the sum of deformed Coulomb and deformed nuclear proximity potentials, for various $E_{\text{c.m.}}$ values. The computed results have been compared with the available experimental data of total cross section corresponding to $E_{\text{c.m.}} = 60.5$ and 51.6 MeV for the entrance channel ^{32}S + ^{24}Mg, which were found to be in good agreement. The experimental values for the LP production cross section and IMF cross section for the channel ^{32}S + ^{24}Mg were also found to agree with our calculations. Hence we have extended our studies and have thus computed the total cross section, IMF cross section, and LP cross section for the decay of ^{56}Ni* formed through the other three entrance channels ^{36}Ar + ^{20}Ne, ^{40}Ca + ^{16}O, and ^{28}Si + ^{28}Si with different $E_{\text{c.m.}}$ values. Hence, we hope that our predictions on the evaluations of the IMF cross sections and the LP cross sections for the decay of ^{56}Ni* formed through these three channels can be used for further experimental studies.

DOI: 10.1103/PhysRevC.95.064607

I. INTRODUCTION

There have been extensive studies on the compound nuclei (CN) formed in the mass region $40 \leqslant A_{\text{CN}} \leqslant 80$ through low-energy reactions [1]. In these fusion-fission reactions, these systems possess considerable fission components in addition to the light-particle evaporation. Theoretically, the deexcitation of the CN through the emission of light particles (LPs) with $A \leqslant 4$ and $Z \leqslant 2$ (n,p,α) and/or γ radiation as well as the intermediate mass fragments (IMFs) or complex fragments have been studied in the past three decades using various models [2–10]. Apparently, the decay process must depend on temperature and angular momentum dependent potential barriers [1]. In the past few years, there have been several experimental and theoretical studies on the decay of light compound nuclear systems formed through heavy-ion reactions [11–15]. The presence of a shell stabilized, highly deformed configuration in compound systems such as ^{48}Cr* and ^{56}Ni* has been indicated through the strong resonance-like structures observed in elastic and inelastic excitation functions of ^{24}Mg + ^{24}Mg [16] and ^{28}Si + ^{28}Si [15], respectively.

Experimentally, the ^{56}Ni compound system was extensively studied by using different entrance channels, namely, ^{16}O + ^{40}Ca, ^{28}Si + ^{28}Si, and ^{32}S + ^{24}Mg, and at various incident energies ranging from 1.5 to 2.2 times the Coulomb barrier [1]. The incident flux is found to get trapped by the formation of a compound nucleus (CN), which is in addition to a significant large-angle elastic scattering cross section at such incident energies. For somewhat heavier systems, such as ^{48}Cr* and ^{56}Ni*, significant decay strength to $A > 4$ fragments (the mass-asymmetric channels) is also observed, which could apparently not arise from a direct reaction mechanism because of the large mass asymmetry differences between the entrance and exit channels. The measured angular distributions and energy spectra are consistent with fission-like decays of the respective compound systems.

^{56}Ni would decay only if it were produced in heavy ion reactions with sufficient compound nucleus excitation energy. Large structure effects have been shown to be important in the ^{56}Ni compound system through a strong resonance behavior [16,17] of the excitation functions of large-angle ^{28}Si + ^{28}Si elastic and inelastic scattering yields [18,19]. Although neither similar resonant effects nor orbiting processes [20] have been evidenced in the ^{32}S + ^{24}Mg reaction [11,21,22], a fully dynamical theory for more complete description of the emission of both the LPs and IMFs within the framework of the statistical model of the decay of such a hot and rotating nuclear ^{56}Ni* system remains highly desirable. In the statistical Hauser-Feshbach analysis [8–10] the evaporation residue has been understood as the equilibrated compound nucleus emission for the production of light particles ($A \leqslant 4$). In the statistical fission models [23,24], the phase space available at the "transition" configuration, which is saddle or scission, determines the fission decay of a compound nucleus. In the saddle-point "transition state" model [9,18,25] the intermediate mass fragments (IMFs) emission has been treated as the binary fission of the compound nucleus. In the present work a different approach has been adopted in which we have considered the collective clusterization (formation) of LPs, IMFs, etc. in the compound nucleus (CN) and the penetration of these clusters through the barrier. The cluster formation probability depends on the size of the cluster, and in the fission model it is calculated as the penetrability of the internal part (overlap region) of the barrier [26,27].

In one of the experiments [9,11] for the ^{32}S + ^{24}Mg → ^{56}Ni* reaction, the mass spectra for $A = 12 - 28$ fragments and the total kinetic energy (TKE) for only the most favored (enhanced yields) α-nucleus fragments are measured at the energies $E_{\text{lab}} = 121.1$ and 141.8 MeV, or equivalently, at

*Corresponding author: drkpsanthosh@gmail.com

$E_{c.m.} = 51.6$ and 60.5 MeV, respectively. In another experiment [28] for the $^{32}S + ^{24}Mg$ reaction the excitation energy for only the symmetric channel $^{28}Si + ^{28}Si$ and near symmetric channel $^{24}Mg + ^{32}S$ were measured at $E_{c.m.} = 51.0$ and 54.5 MeV, which on analysis indicate that specific set of states in ^{28}Si correspond to highly deformed bands. In a recent experiment [29] for the same reaction $^{32}S + ^{24}Mg$, the incident energy used was $E_{lab} = 130$ MeV and an enhanced emission yield by a factor of 1.5–1.8 was observed for ^{8}Be over two α particles. Sanders *et al.* [30] determined the inclusive cross sections for the $^{16}O + ^{40}Ca$ reaction leading to fission-like fragments with mass $20 \leqslant A_{frag} \leqslant 28$, and for the $^{16}O + ^{44}Ca$ reaction with $20 \leqslant A_{frag} \leqslant 30$, at seven energies with $69.3 \leqslant E_{lab}(^{16}O) \leqslant 87.3$ MeV and for $30^\circ \leqslant \theta_{lab} \leqslant 60^\circ$. Beck *et al.* [19] undertook a high-resolution measurement of fragment-fragment γ triple coincidence events in the symmetric and near-symmetric mass exit channels from the $^{28}Si + ^{28}Si$ reaction using the EUROGAM Phase II γ-ray spectrometer. Gomez del Campo [31] experimentally measured the cross sections for the reaction $^{58}Ni + ^{58}Ni$ in their ground and excited states at a bombarding energy of 630 MeV. Gary *et al.* [32] measured the complete fusion or residue distributions for the ^{24}Mg, $^{28}Si + ^{12}C$, $^{24}Mg + ^{24,26}Mg$, $^{28}Si + ^{24}Mg$, and $^{28,29,30}Si$ systems with several experimental techniques for a wide range of energies which spread from 1 to 3 times the Coulomb barrier (21–42 MeV).

A recent attempt of dynamically treating the decay of a hot and rotating nucleus formed in heavy-ion reaction was made by Gupta and collaborators [33–38]. Gupta *et al.* [35,39] studied the decay of $^{56}Ni^*$ formed in the $^{32}S + ^{24}Mg$ reaction at two incident energies $E_{c.m.} = 51.6$ and 60.5 MeV using the dynamical cluster decay model (DCM). Karthikraj *et al.* [40] studied the decay of odd-A and non-α structured $^{59}Cu^*$ formed in the $^{35}Cl + ^{24}Mg$ reaction at $E_{lab} = 275$ MeV, applying the reformulated dynamical cluster decay model. One of us (K.P.S.), studied the heavy-ion fusion cross section and barrier distributions for ^{12}C, ^{16}O, ^{28}Si, and ^{35}Cl on ^{92}Zr [41] and that of weakly bound ^{9}Be on ^{27}Al and ^{64}Zn, tightly bound ^{16}O on a ^{64}Zn target [42], and ^{16}O on spherical/deformed $^{144-154}Sm$ targets [43] within the barrier penetration model, taking the scattering potential as the sum of Coulomb and nuclear proximity potential of Blocki *et al.* [44,45]. Within the same model, the probable-target combinations for the synthesis of the super heavy nucleus $^{302}120$ [46] also have been studied. Recently, the decay properties of various even-even isotopes of Ba [47] and the decay of the excited compound system $^{48}Cr^*$ formed through $^{24}Mg + ^{24}Mg$, $^{36}Ar + ^{12}C$, and $^{20}Ne + ^{28}Si$ reactions was studied by Santhosh *et al.* [48]. In the present manuscript, we have performed an extensive study on the total cross section, the production cross section of IMF, and the light particle (LP) formation cross section of $^{56}Ni^*$ formed through the channels $^{32}S + ^{24}Mg$, $^{36}Ar + ^{20}Ne$, $^{40}Ca + ^{16}O$, and $^{28}Si + ^{28}Si$ at various $E_{c.m.}$ values using Wong's formula [49], the Glas and Mosel formula [50] by incorporating the temperature-dependent diffuseness parameter, and the radius for the nucleus-nucleus potential taken from Royer *et al.* [51], taking the scattering potential as the sum of the deformed Coulomb and deformed nuclear proximity potentials. Here, the total cross section, the IMF production cross section, and the LP cross sections are calculated for all the entrance channels using the ℓ-summed Wong formula for cross section, the approximated Wong formula for relatively large values of E, and using the Glas and Mosel formula for cross sections for the deformed nuclei. For the entrance channel $^{32}S + ^{24}Mg$, the experimental data [9,11] are available for total cross section, LP and IMF production cross sections corresponding to $E_{c.m.} = 60.5$ and 51.6 MeV. A comparison of the computed values with the available experimental data [9,11] is found to show good agreement. Hence we have extended our studies and calculated the total cross section, LP production cross section, and IMF cross sections for the other three channels $^{36}Ar + ^{20}Ne$, $^{40}Ca + ^{16}O$, and $^{28}Si + ^{28}Si$, which can help future experimental studies on $^{56}Ni^*$.

The details of the formalisms used for the evaluation of the scattering potential, the sum of Coulomb and proximity potentials, and formalisms used for the evaluation of production cross section are presented in Sec. II. In Sec. III, we present the results and discussion of the study, and a conclusion of the entire work is given in Sec. IV.

II. THEORY

A. The potential

The cross section measurements were made by taking the scattering potential as the sum of Coulomb and proximity potentials of Blocki *et al.* [44,45]. A simple formula for the nucleus-nucleus interaction as a function of separation between the surfaces of the approaching nuclei is given by the proximity potential. The formula uses measured values of nuclear surface tension and surface diffuseness and is free from adjustable parameters. The interaction potential energy barrier for spherical fragments, which is the sum of Coulomb potential, proximity potential, and centrifugal potential, is given as

$$V = \frac{Z_1 Z_2 e^2}{r} + V_P(z) + \frac{\hbar^2 \ell(\ell+1)}{2\mu r^2}, \quad \text{for z} > 0. \tag{1}$$

Here Z_1 and Z_2 are the atomic numbers of the interacting fragments, the distance between the centers of the interacting fragments is given by r, z is the distance between the near surface of the fragments, and ℓ is the angular momentum. μ is the reduced mass which is given as $\mu = mA_1A_2/A$ where m is the mass of the nucleon and A, A_1, and A_2 are the mass numbers of the compound nucleus and the interacting fragments respectively. The proximity potential V_p is given by Blocki *et al.* [44]:

$$V_p(z) = 4\pi\gamma b \frac{C_1 C_2}{C_1 + C_2} \phi\left(\frac{z}{b}\right). \tag{2}$$

Here, $r = z + C_1 + C_2$, where C_1 and C_2 are the Süssman central radii. The nuclear surface tension coefficient is given as

$$\gamma = 0.9517[1 - 1.7826(N - Z)^2/A^2], \tag{3}$$

where N and Z are neutron and proton numbers of parent nuclei. The universal proximity potential ϕ is given as [45]

$$\phi(\varepsilon) = -4.41e^{\frac{-\varepsilon}{0.7176}} \quad \text{for } \varepsilon > 1.9475, \tag{4}$$

$$\phi(\varepsilon) = -1.7817 + 0.9270\varepsilon + 0.0169\varepsilon^2 - 0.05148\varepsilon^3 \quad \text{for } 0 \leqslant \varepsilon \leqslant 1.9475, \tag{5}$$

with $\varepsilon = z/b$ and the Süssman central radii C_i is related to sharp radii R_i as $C_i = R_i - \frac{b^2}{R_i}$ and $b \sim 1$ fm is the surface width. When effect of temperature T is included, the surface width changes as [51]

$$b(T) = 0.99[1 + 0.009T^2]. \tag{6}$$

The Süsmann central radii [51] will be reformulated for the inclusion of temperature T as

$$C_i = R_i(T) - \frac{0.99[1 + 0.009T^2]^2}{R_i(T)}. \tag{7}$$

The semiempirical formula in terms of mass number A_i for R_i is given as

$$R_i = 1.28A_i^{1/3} - 0.76 + 0.8A_i{}^{-1/3}. \tag{8}$$

For an excited compound system the semiempirical formula can be written as

$$R_i(T) = \left[1.28A_i{}^{1/3} - 0.76 + 0.8A_i{}^{-1/3}\right][1 + 0.0007T^2]. \tag{9}$$

The barrier penetrability P for an excited compound system is given as

$$P = \exp\left\{-\frac{2}{\hbar}\int_a^b \sqrt{2\mu(V - Q_{\text{eff}})}dz\right\} \tag{10}$$

with $V(a) = V(b) = Q_{\text{eff}}$, the effective Q value; Q_{eff} is given as

$$Q_{\text{eff}} = Q + E^*. \tag{11}$$

The excitation energy E^* and the nuclear temperature T (in MeV) [52] are related as

$$E^* = \tfrac{1}{9}AT^2 - T. \tag{12}$$

The Coulomb interaction between the two deformed and oriented nuclei, which is taken from [42] and which includes higher multipole deformation [53–56], is given as

$$V_C = \frac{Z_1Z_2e^2}{r} + 3Z_1Z_2e^2 \sum_{\lambda,i=1,2} \frac{1}{2\lambda+1}\frac{R_i^\lambda(\alpha_i)}{r^{\lambda+1}}Y_\lambda^{(0)}(\theta_i) \times \left[\beta_{\lambda i} + \frac{4}{7}\beta_{\lambda i}^2 Y_\lambda^{(0)}(\theta_i)\delta_{\lambda,2}\right] \tag{13}$$

with

$$R_i(\alpha_i) = R_{0i}\left[1 + \sum_\lambda \beta_{\lambda i}Y_\lambda^{(0)}(\alpha_i)\right], \tag{14}$$

where $R_{0i}(T) = [1.28A_i{}^{1/3} - 0.76 + 0.8A_i{}^{-1/3}][1 + 0.0007T^2]$. Here θ_i is the angle between the symmetry axis of the deformed nuclei and the line joining the centers of the two interacting nuclei, α_i is the angle between the radius vector and symmetry axis of the ith nuclei (see Fig. 1 of Ref, [54]), and the quadrupole interaction term proportional to $\beta_{21}\beta_{22}$, which is due to its short-range character, is neglected.

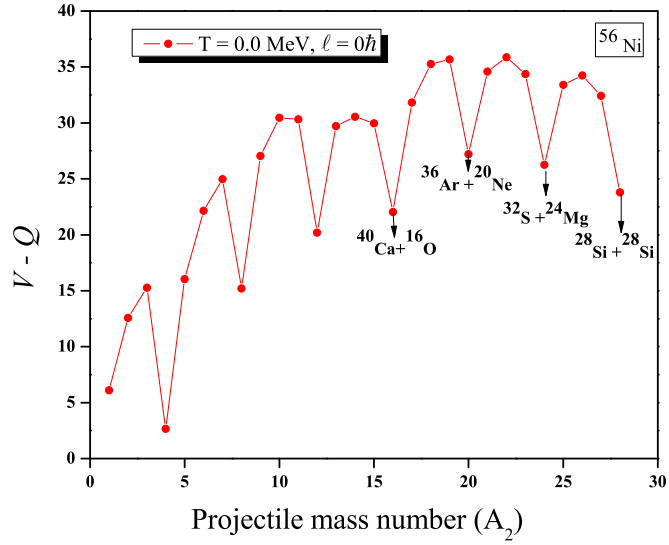

FIG. 1. Cold reaction valley plot of ^{56}Ni.

The deformation comes only in the mean curvature radius for the proximity potential, $V_P(z) = 4\pi\gamma b\bar{R}\Phi(\varepsilon)$. The mean curvature radius is defined as $\bar{R} = \frac{C_1C_2}{C_1+C_2}$ for spherical nuclei, where C_1 and C_2 are Süssmann central radii of fragments. The mean curvature radius $\bar{R}$ of two deformed nuclei lying in the same plane can be evaluated by the relation [54]

$$\frac{1}{\overline{R}^2} = \frac{1}{R_{11}R_{12}} + \frac{1}{R_{21}R_{22}} + \frac{1}{R_{11}R_{22}} + \frac{1}{R_{21}R_{12}}, \tag{15}$$

where the four principal radii of curvature R_{i1} and R_{i2}, with $i = 1,2$, at the two points D and E (see Fig. 1 of Ref [54]) of closest approach of the interacting nuclei are given by Baltz and Bayman [57] as

$$R_{i1} = \left|\frac{\left\{R_i^2(\alpha_i) + [R'_i(\alpha_i)]^2\right\}^{3/2}}{R''_i(\alpha_i)R_i(\alpha_i) - 2[R'_i(\alpha_i)]^2 - R_i^2(\alpha_i)}\right|, \tag{16}$$

$$R_{i2} = \left|\frac{R_i(\alpha_i)\sin\alpha_i\left[R_i^2(\alpha_i) + (R'_i(\alpha_i))^2\right]^{1/2}}{R'_i(\alpha_i)\cos\alpha_i - R_i(\alpha_i)\sin\alpha_i}\right|, \tag{17}$$

where, $R'(\alpha)$ and $R''(\alpha)$ are the first and second derivatives of $R(\alpha)$ with respect to α, respectively.

B. Decay cross section of the compound nucleus (CN)

The interaction barrier for the s wave, traditionally referred to as the "Coulomb barrier," has been of great interest, and Wong [49] obtained a method to measure this barrier by employing a simple analytic expression for the total reaction cross section obtained in the ingoing-wave strong-absorption model. Later, following Thomas [58], Huizenga *et al.*, [59] and Ramussen *et al.*, [60], Wong, employing the inverted harmonic potentials of height E and frequency ω_ℓ, approximated the various barriers for different partial waves. Using the probability for absorption of the ℓth partial wave given by

the Hill-Wheeler formula [61], Wong arrived at the total cross section by quantum mechanical penetration of the potential barrier for an energy E_ℓ, which is given as

$$\sigma = \frac{\pi}{k^2}\sum_{\ell}\frac{2\ell+1}{1+\exp[2\pi(E_\ell - E)/\hbar\omega_\ell]}, \tag{18}$$

where $k = \sqrt{\frac{2\mu E}{\hbar^2}}$. Here E is the excitation energy of the compound nucleus, $\hbar\omega_\ell$ is the curvature of the inverted parabola, and E_ℓ is the interaction barrier for the ℓth partial wave:

$$\hbar\omega_\ell = \hbar\left[\left.\frac{d^2V(r)}{dr^2}\right|_{R_\ell}\Big/\mu\right]^{1/2}. \tag{19}$$

Here, radial separation R_ℓ is obtained from the condition

$$\left.\frac{d^2V(r)}{dr^2}\right|_{R_\ell} = 0. \tag{20}$$

In the region of $\ell = 0$, using some parametrizations,

$$E_\ell \cong E_0 + \frac{\hbar^2\ell(\ell+1)}{2\mu R_0^2}, \tag{21}$$

$$\hbar\omega_\ell \cong \hbar\omega_0. \tag{22}$$

Wong derived the cross section by using (21) and (22) and replacing the sum in Eq. (18) by integration, which is given as

$$\sigma = \frac{R_0^2\hbar\omega_0}{2E}\ln\left\{1+\exp\left[\frac{2\pi(E-E_0)}{\hbar\omega_0}\right]\right\}. \tag{23}$$

For relatively large values of E, the above equation reduces to

$$\sigma = \pi R_0^2\left[1-\frac{E_0}{E}\right]. \tag{24}$$

Lefort and his collaborators showed that for two complex nuclei [62] to interact, not a critical angular momentum but a critical distance of approach may be the relevant quantity. To substantiate the finding of critical approach, it is necessary to check the linear dependence of σ on $1/E$ in the region of higher energies. The critical distance is given as

$$R_c = r_c\left(A_1^{1/3} + A_2^{1/3}\right), \quad r_c = 1.0 \pm 0.07 \text{ fm}. \tag{25}$$

Gutbrod, Winn, and Blann from their analysis of low energy data [63], obtained the interaction distance as

$$R_B = r_B\left(A_1^{1/3} + A_2^{1/3}\right), \quad r_B = 1.4 \text{ fm}, \tag{26}$$

which is found to be larger than R_c by 40% and corresponds to the distance of the ions at the barrier.

In order to understand the difference between the two distances given by Eqs. (25) and (26), Glas and Mosel [50] set σ as

$$\sigma = \pi\lambda^2\sum_{\ell=0}^{\infty}(2\ell+1)T_i P_i, \tag{27}$$

where P_i gives the probability for reaction to take place once the barrier has been passed ($P_i = 1$ for $\ell \leqslant \ell_c$ and $P_i = 0$ for $\ell > \ell_c$) and T_i is the penetration probability through the interaction barrier. Approximating the frequencies $\hbar\omega_\ell$ and the position of the interaction barrier by constant values $\hbar\omega$ and R_B respectively, and then replacing the sum in Eq. (25) by integration, the expression for σ is obtained as

$$\sigma = \frac{\hbar\omega}{2}R_B^2\frac{1}{E}\ln\left\{\frac{1+\exp[2\pi\{E-V(R_B)\}/\hbar\omega]}{1+\exp[2\pi\{E-V(R_B)-(R_C/R_B)^2[E-V(R_C)]\}/\hbar\omega]}\right\} \tag{28}$$

For oriented nuclei, the decay cross sections σ depend on the orientation angle θ, hence here in the present calculations we have evaluated the decay cross sections for different orientations, and we got $\sigma(E_{\text{c.m.}})$ on integrating over the angles θ_i.

III. RESULT AND DISCUSSIONS

^{56}Ni, being a negative Q value system, should be produced with sufficient compound nucleus excitation energy (E^*_{CN}) by a heavy ion reaction for it to decay. The concept of a cold reaction valley is related to the minima in the so-called driving potential, which is defined as the difference between the interaction potential V and the Q value of the reaction. The driving potential of the compound nucleus is computed for all possible combinations of projectile and target for the touching configuration of the two. The most probable combinations for the formation of CN are represented as the minima in the driving potential which are due to shell closure of projectile or target or both. The entrance channel ^{32}S + ^{24}Mg for the formation of the ^{56}Ni compound nucleus has been experimentally determined [9,11], but the other possible projectile-target combinations for the formation of ^{56}Ni were found from the cold reaction valley plot. The cold reaction valley plot of ^{56}Ni is shown in Fig. 1, where the projectile mass number A_2 is taken along the X axis and the driving potential $V - Q$ is taken along Y axis corresponding to $T = 0.0$ MeV and $\ell = 0$.

Figure 2 represents the plot of $V - Q_{\text{eff}}$ vs fragment mass number, which corresponds to the exit channels for the decay of ^{56}Ni*. The potential V is found to depend on the distance between the fragment centers r, where $r = z + C_1 + C_2$, where C_1 and C_2 are the Süssman central radii of fragments and z is the distance between the near surfaces of the fragments. The plot corresponds to two different experimental $E_{\text{c.m.}}$ values, 51.6 MeV ($T = 3.327$ MeV) and 60.5 MeV ($T = 3.541$ MeV) with corresponding ℓ_c values. It can be

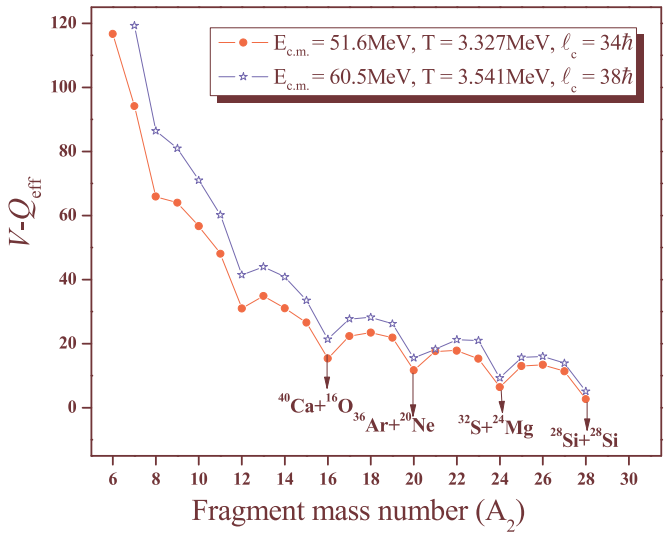

FIG. 2. The driving potential as a function of the mass number of one of the fragments, A_2, for the system ^{56}Ni*.

seen from the figure that the structure of the potential remains unchanged with the increase in $E_{\text{c.m.}}$ values and with increase in ℓ values. The effective Q value, Q_{eff}, is found to increase with increase in $E_{\text{c.m.}}$ value [from Eq. (11)] but the driving potential $V - Q_{\text{eff}}$ is found to be larger for higher $E_{\text{c.m.}}$ because the interaction potential V depends on the temperature dependent Coulomb potential, temperature dependent nuclear potential, and temperature dependent centrifugal potential.

The LP ($A \leqslant 4$) emissions are energetically more favorable at lower energies (lower ℓ values), i.e., σ_{LP} is the cross section obtained by summing over the cross section from $\ell = 0$ to $\ell = \ell_c$. The emission of IMFs ($A > 4$) begins only beyond a certain ℓ value (where the cross section has the maximum value), and the cross section σ_{IMF} is found to be maximum for $\ell = \ell_c$. The critical angular momentum value ℓ_c was calculated from the condition that the effective radial potential $V(r,\ell)$, which is the sum of Coulomb, nuclear, and centrifugal potentials, reaches a local maximum equal to the incoming center-of-mass energy $E_{\text{c.m.}}$:

$$V(r,\ell) = E_{\text{c.m.}}, \quad \frac{\partial V(r,\ell)}{\partial r} = 0, \quad \text{for } \ell = \ell_c, \quad r = R_m. \tag{29}$$

Here R_m is the separation distance at which the radial potential reaches a local maximum, corresponding to critical angular momentum. The experimental values are available only for the channel $^{32}\text{S} + ^{24}\text{Mg}$, but the other channels for the formation of compound nucleus have been chosen from the cold valley plot (Fig. 1). For all the four channels $^{32}\text{S} + ^{24}\text{Mg}$, $^{36}\text{Ar} + ^{20}\text{Ne}$, $^{40}\text{Ca} + ^{16}\text{O}$ and $^{28}\text{Si} + ^{28}\text{Si}$ we have plotted the variation of the interaction barrier with distance between the centers of fragments, and hence the values of E_B and R_B for the calculations of total cross section were determined. The total cross sections, with the inclusion of deformations, were calculated using the ℓ-summed Wong formula, Eq. (18), the approximated Wong formula for relatively large values of E, Eq. (24), and the Glas and Mosel formula for cross section, Eq. (28). The total cross section, IMF production cross section, and light particle production cross sections were calculated separately by taking into account the temperature effects. Even though, the total cross section is theoretically given by $\sigma_{\text{Total}} = \sigma_{LP} + \sigma_{\text{IMF}}$, the values of cross sections evaluated using our model show a slight difference so that the total cross section σ_{Total} is not exactly the sum of light particle production cross section and IMF production cross section, $\sigma_{LP} + \sigma_{\text{IMF}}$. The total production cross sections (σ_{Total}) thus obtained for various center-of-mass energies ($E_{\text{c.m.}}$) values have been compared with the experimental data [9,11], as shown in Table I. The behavior of LPs and IMFs are very different. Also lower ℓ's contribute to LP cross section (σ_{LP}) and higher ℓ's to fission-like IMF cross section (σ_{IMF}). The experimental total cross section, IMF production cross section, and LP cross section for the channel $^{32}\text{S} + ^{24}\text{Mg}$ corresponding to $E_{\text{c.m.}}$ of 60.5 MeV are 1125.64, 75.640, and 1050 $\pm$ 100 mb respectively. The values computed using our formalisms for the total cross section, production cross section of IMF, and light particle formation cross section are 1244.648, 80.783, and 1162 mb respectively for the entrance channel $^{32}\text{S} + ^{24}\text{Mg}$ at $E_{\text{c.m.}} = 60.5$ MeV. Also corresponding to an $E_{\text{c.m.}}$ of 51.6 MeV, the above cross sections have the experimental values 1139 $\pm$ 142, 59 $\pm$ 12, and 1080 $\pm$ 130 mb respectively for the same channel. Our calculations for the same channel at $E_{\text{c.m.}} = 51.6$ MeV give the values of cross sections 1211.323, 52.550, and 1158 mb respectively. An analysis of the result shows that the total cross section, production cross section of IMF, and light particle formation cross section calculated using the present model are in close agreement with experimental values [9,11]. The experimental total cross section is found to show close agreement with the values computed using the Glas and Mosel formula. Hence we have extended our studies and evaluated the total cross section, IMF production cross section, and LP cross section for the other three channels $^{36}\text{Ar} + ^{20}\text{Ne}$, $^{40}\text{Ca} + ^{16}\text{O}$, and $^{28}\text{Si} + ^{28}\text{Si}$ for various $E_{\text{c.m.}}$ values. The computed values are shown in Table I. The first column indicates the entrance channel of ^{56}Ni*. The second and the third columns gives the $E_{\text{c.m.}}$ values and the critical angular momentum ℓ_c corresponding to each $E_{\text{c.m.}}$. The experimental total production cross section for the channel $^{32}\text{S} + ^{24}\text{Mg}$ corresponding to the $E_{\text{c.m.}}$ values 60.5 and 51.6 MeV are given in column 4. The total cross sections, with the inclusion of deformations which were calculated using the ℓ-summed Wong formula, Eq. (18), approximated Wong formula for relatively large values of E, Eq. (24), and the Glas and Mosel formula for cross section, Eq. (28), are given in columns 5, 6, and 7 respectively. Column 8 gives the experimental IMF production cross section for the channel $^{32}\text{S} + ^{24}\text{Mg}$ corresponding to the $E_{\text{c.m.}}$ values of 60.5 and 51.6 MeV. The IMF cross section calculated using our model is given in the next column. Columns 9 and 10 give the experimental LP production cross section for the channel $^{32}\text{S} + ^{24}\text{Mg}$ and the LP production cross section calculated using our model, respectively.

TABLE I. The computed cross sections σ_{Total}, σ_{IMF}, σ_{LP} for the decay of ^{56}Ni* formed through ^{24}Mg + ^{24}Mg, ^{36}Ar + ^{20}Ne, ^{40}Ca + ^{16}O, and ^{28}Si + ^{28}Si channels and comparison with experimental data [9,11].

Entrance channel	$E_{\text{c.m.}}$ (MeV)	ℓ_c (ħ)	σ_{Total}				σ_{IMF}		σ_{LCP}	
			Expt. (mb)	Eq. (18) (mb)	Eq. (24) (mb)	Eq. (28) (mb)	Expt. (mb)	Theor. (mb)	Expt. (mb)	Theor. (mb)
	70.0	42		1962.889	1962.889	1270.869		264.361		1005
	65.0	40		1875.196	1875.196	1258.024		191.256		1067
	60.5	38	1125.64	1783.880	1783.880	1244.648	75.640	80.783	1050 ± 100	1162
^{32}S + ^{24}Mg	55.0	36		1651.979	1651.979	1225.327		60.830		1164
	51.6	34	1139 ± 142	1556.376	1556.376	1211.323	59 ± 12	52.550	1080 ± 130	1158
	45.0	30		1329.554	1329.554	1178.098		22.432		1022
	40.0	26		1107.886	1107.886	1106.407		13.101		828
	70	38		1497.368	1497.368	1285.573		212.919		1072
	65	36		1425.661	1425.661	1275.401		237.142		1038
	60	34		1342.003	1342.003	1263.533		258.587		1005
^{36}Ar + ^{20}Ne	55	32		1243.134	1243.134	1238.224		275.073		960
	50	30		1124.491	1124.491	1124.491		242.603		885
	45	28		979.484	979.484	979.484		162.281		815
	40	26		798.224	798.224	798.224		13.751		785
	70	37		1271.444	1271.444	1271.444		380.253		890
	65	36		1213.076	1213.076	1213.076		348.579		865
	60	34		1144.981	1144.981	1144.981		294.794		850
^{40}Ca + ^{16}O	55	32		1064.505	1064.505	1064.505		254.585		810
	50	30		967.933	967.933	967.933		212.268		755
	45	28		849.901	849.901	849.901		162.905		685
	40	26		702.361	702.361	702.361		54.438		645
	70	38		1045.619	1045.619	1045.619		280.254		765
	65	36		977.129	977.129	977.129		298.258		680
	60	34		897.225	897.225	897.225		312.731		585
^{28}Si + ^{28}Si	55	32		802.792	802.792	802.792		293.711		510
	50	30		689.173	689.173	689.173		249.461		440
	45	28		550.972	550.972	550.972		123.050		425
	40	24		377.846	377.846	377.846		90.081		285

IV. CONCLUSIONS

The decay of ^{56}Ni*, formed through various entrance channels ^{32}S + ^{24}Mg, ^{36}Ar + ^{20}Ne, ^{40}Ca + ^{16}O, and ^{28}Si + ^{28}Si has been studied using the ℓ-summed Wong formula, the approximated Wong formula for relatively large values of E, and the Glas and Mosel formula for cross section. The total cross section, the intermediate mass fragment (IMF) production cross section, and the cross section for the formation of light particles (LPs) have been evaluated for the deformed nuclei. The computed results on the total cross section and LP production cross section for the entrance channel ^{32}S + ^{24}Mg have been compared with the available experimental data and were found to be in good agreement. Hence we have studied the total cross section, IMF cross section, and LP cross section for the decay of ^{56}Ni* formed through other entrance channels ^{36}Ar + ^{20}Ne, ^{40}Ca + ^{16}O, and ^{28}Si + ^{28}Si with different $E_{\text{c.m.}}$ values. Hence, we hope that our predictions on the evaluations of the IMF cross sections and the light charged particle cross sections for the decay of ^{56}Ni* formed through the three entrance channels ^{36}Ar + ^{20}Ne, ^{40}Ca + ^{16}O, and ^{28}Si + ^{28}Si can be used for further experimental studies.

[1] S. J. Sanders, A. Szanto de Toledo, and C. Beck, Phys. Rep. **311**, 487 (1999).

[2] N.V. Antonenko, S. P. Ivanova, R. V. Jolos, and W. Scheid, Phys. Rev. C **50**, 2063 (1994).

[3] G. G. Adamian, N. V. Antonenko, and W. Scheid, Phys. Rev. C **68**, 034601 (2003).

[4] Sh. A. Kalandarov, G. G. Adamian, N.V. Antonenko, W. Scheid, and J. P. Wieleczko, Phys. Rev. C **84**, 064601 (2011).

[5] G. Adamian, N. Antonenko, and W. Scheid, in *Clusters in Nuclei*, Lecture Notes in Physics Vol. 848, edited by C. Beck, Vol. 2 (Springer, Berlin, 2012), p. 165.

[6] G. Royer, C. Bonilla, and R. A. Gherghescu, Phys. Rev. C **67**, 034315 (2003).

[7] R. A. Gherghescu and G. Royer, Phys. Rev. C **68**, 014315 (2003).

[8] R. J. Charity *et al.*, Nucl. Phys. A **476**, 516 (1988); **483**, 371 (1988).

[9] S. J. Sanders, D. G. Kovar, B. B. Back, C. Beck, D. J. Henderson, R. V. F. Janssens, T. F.Wang, and B. D. Wilkins, Phys. Rev. C **40**, 2091 (1989).

[10] T. Matsuse, C. Beck, R. Nouicer, and D. Mahboub, Phys. Rev. C **55**, 1380 (1997).

[11] S. J. Sanders, D. G. Kovar, B. B. Back, B. K. Dichter, D. Henderson, R. V. F. Jansens, J. G. Kerllers, S. Kaufman, T. F. Wang, B. Wilkins, and F. Videbaek, Phys. Rev. Lett. **59**, 2856 (1987).

[12] C. Beck, B. Djerroud, B. Heusch, R. Dayras, R. M. Freeman, F. Haas, A. Hachem, J. P. Wieleczko, and M. Youlal, Z. Phys. A **334**, 521 (1989).

[13] A. Ray, D. Shapira, J. Gomez del Campo, H. J. Kim, C. Beck, B. Djerroud, B. Heusch, D. Blumenthal, and B. Shivakumar, Phys. Rev. C **44**, 514 (1991).

[14] C. Bhattacharya, D. Bandyopadhyay, S. K. Basu, S. Bhattacharya, K. Krihsam, G. S. N. Murthy, A. Chatterjee, S. Keilas, and P. Singh, Phys. Rev. C **54**, 3099 (1996).

[15] R. R. Betts, H.-G. Clerc, B. B. Back, I. Ahmed, K. L. Wolf, and B. G. Glagola, Phys. Rev. Lett. **46**, 313 (1981).

[16] C. Beck, Y. Abe, N. Aissaoui, B. Djerroud, and F. Haas, Phys. Rev. C **49**, 2618 (1994).

[17] C. Beck, Y. Abe, N. Aissaoui, B. Djerroud, and F. Haas, Nucl. Phys. A **583**, 269 (1995).

[18] R. Nouicer, C. Beck, R. M. Freeman, F. Haas, N. Aissaoui, T. Bellot, G. de France, D. Disdier, G. Duchˆene, A. Elanique, A. Hachem, F. Hoellinger, D. Mahboub, V. Rauch, S. J. Sanders, A. Dummer, F. W. Prosser, A. Szanto de Toledo, Sl. Cavallaro, E. Uegaki, and Y. Abe, Phys. Rev. C **60**, 041303 (1999).

[19] C. Beck, R. Nouicer, D. Disdier, G. Duchˆene, G. de France, R. M. Freeman, F. Haas, A. Hachem, D. Mahboub, V. Rauch, M. Rousseau, S. J. Sanders, and A. Szanto de Toledo, Phys. Rev. C **63**, 014607 (2000).

[20] D. Shapira, Phys. Rev. Lett. **61**, 2153 (1988).

[21] S. J. Sanders, D. G. Kovar, B. B. Back, C. Beck, B. K. Dichter, D. Henderson, R. V F. Janssens, J. G. Keller, S. Kaufman, T.-F. Wang, B. Wilkins, and F. Videbaek, Phys. Rev. Lett. **61**, 2154 (1988).

[22] S. J. Sanders, B. B. Back, R. V. F. Janssens, D. G. Kovar, D. Habs, D. Henderson, T.-L. Khoo, H. Korner, G.-E. Rathke, T. F. Wang, F. L. H.Wolfs, and K. B. Beard, Phys. Rev. C **41**, R1901 (1990).

[23] L. G. Moretto, Nucl. Phys. A **247**, 211 (1975).

[24] R. Vandenbosch and J. R. Huizenga, *Nuclear Fission* (Academic, New York, 1973).

[25] S. J. Sanders, Phys. Rev. C **44**, 2676 (1991).

[26] D. N. Poenaru, W. Greiner, and E. Hourani, Phys. Rev. C **51**, 594 (1995).

[27] K. P. Santhosh and Antony Joseph, Pramana J. Phys. **59**, 599 (2002).

[28] S. J. Sanders, A. Hasan, F. W. Prosser, B. B. Back, R. R. Betts, M. P. Carpenter, D. J. Henderson, R. V. F. Janssens, T. L. Khoo, E. F. Moore, P. R. Wilt, F. L. H. Wolfs, A. H. Wuosmaa, K. B. Beard, and Ph. Benet, Phys. Rev. C **49**, 1016 (1994).

[29] S. Thummerer, W. von Oertzen, B. Gebauer, S.M. Lenzi, A. Gadea, D. R. Napoli, C. Beck, and M. Rousseau, J. Phys. G: Nucl. Part. Phys. **27**, 1405 (2001).

[30] S. J. Sanders, R. R. Betts, I. Ahmad, K. T. Lesko, S. Saini, and B. D. Wilkins, Phys. Rev. C **34**, 1746 (1986).

[31] J. Gomez del Campo, R. L. Auble, J. R. Beene, M. L. Halbert, H. J. Kim, A. D'Onofrio, and J. L. Charvet, Phys. Rev. C **43**, 2689 (1991).

[32] S. Gary and C. Volant, Phys. Rev. C **25**, 1877 (1982).

[33] M. K. Sharma, R. K. Gupta, and W. Scheid, J. Phys. G: Nucl. Part. Phys. **26**, L45 (2000).

[34] R. K. Gupta, M. Balasubramaniam, C. Mazzocchi, M. La Commara, and W. Scheid, Phys. Rev. C **65**, 024601 (2002).

[35] R. K. Gupta, R. Kumar, N. K. Dhiman, M. Balasubramaniam, W. Scheid, and C. Beck, Phys. Rev. C **68**, 014610 (2003).

[36] M. Balasubramaniam, R. Kumar, R. K. Gupta, C. Beck, and W. Scheid, J. Phys. G: Nucl. Part. Phys. **29**, 2703 (2003).

[37] R. K. Gupta, Acta Phys. Hung. (N. S.) Heavy Ion Phys. **18**, 347 (2003).

[38] R. K. Gupta, M. Balasubramaniam, R. Kumar, D. Singh, and C. Beck, Nucl. Phys. A **738**, 479 (2004).

[39] R. K. Gupta, M. Balasubramaniam, R. Kumar, D. Singh, C. Beck, and W. Greiner, Phys. Rev. C **71**, 014601 (2005).

[40] C. Karthikraj and M. Balasubramaniam, Phys. Rev. C **87**, 024608 (2013).

[41] K. P. Santhosh, V. Bobby Jose, A. Joseph, and K. M. Varier, Nucl. Phys. A **817**, 35 (2009).

[42] K. P. Santhosh and V. Bobby Jose, Nucl. Phys. A **922**, 191 (2014).

[43] K. P. Santhosh and V. Bobby Jose, Rom. Rep. Phys. **66**, 939 (2014).

[44] J. Blocki, J. Randrup, W. J. Swiatecki, and C. F. Tsang, Ann. Phys. (NY) **105**, 427 (1977).

[45] J. Blocki and W. J. Swiatecki, Ann. Phys. (NY) **132**, 53 (1981).

[46] K. P. Santhosh and V. Safoora, Phys. Rev. C **94**, 024623 (2016).

[47] K. P. Santhosh, P. V. Subha, and B. Priyanka, Pramana J. Phys. **86**, 819 (2015).

[48] K. P. Santhosh, P. V. Subha, and B. Priyanka, Eur. Phys. J. A **52**, 125 (2016).

[49] C.Y. Wong, Phys. Rev. Lett. **31**, 766 (1973).

[50] D. Glas and U. Mosel, Phys. Rev. C **10**, 2620 (1974).

[51] G. Royer and J. Mignen, J. Phys. G: Nucl. Part. Phys. **18**, 1781 (1992).

[52] K. J. Le Couteur and D. W. Lang, Nucl. Phys. **13**, 32 (1959).

[53] R. K. Gupta, M. Balasubramaniam, R. Kumar, N. Singh, M. Manhas, and W. Greiner, J. Phys. G: Nucl. Part. Phys. **31**, 631 (2005).

[54] N. Malhotra and R. K. Gupta, Phys. Rev. C **31**, 1179 (1985).

[55] B. V. Carlson, L. C. Chamon, and L. R. Gasques, Phys. Rev. C **70**, 057602 (2004).

[56] N. Takigawa, T. Rumin, and N. Ihara, Phys. Rev. C **61**, 044607 (2000).

[57] A. J. Baltz and B. F. Bayman, Phys. Rev. C **26**, 1969 (1982).

[58] T. D. Thomas, Phys. Rev. **116**, 703 (1959).

[59] J. Huizenga and G. Igo, Nucl. Phys. **29**, 462 (1961).

[60] J. O. Rasmussen and K. Sugawara-Tanabe, Nucl. Phys. A **171**, 497 (1971).

[61] D. L. Hill and J. A. Wheeler, Phys. Rev. **89**, 1102 (1953).

[62] J. Galin, D. Guerreau, M. Lefort, and X. Tarrago, Phys. Rev. C **9**, 1018 (1974).

[63] H. H. Gutbrod, W. G. Winn, and M. Blann, Nucl. Phys. A **213**, 267 (1973).